# Structural and electrochemical properties of aluminium doped $LiMn_2O_4$ cathode materials for Li battery: experimental and *ab initio* calculations

Mesfin A. Kebede[1,a)], Maje J. Phasha[1], Niki Kunjuzwa[1], Lukas J. le Roux[1], Donald Mkhonto[2], Kenneth I. Ozoemena[1] and Mkhulu K. Mathe[1]

[1]*Materials Science and Manufacturing, Council for Scientific and Industrial Research (CSIR), Pretoria, 0001, South Africa*

[2]*Modelling and Digital Science, Council for Scientific and Industrial Research (CSIR), Pretoria, 0001, South Africa*

Pristine and Al-doped lithium manganese oxide ($LiAl_xMn_{2-x}O_4$) spinel cathode materials were successfully synthesized by combustion method using urea as reducer and fuel. The structural and electrochemical properties of the as-synthesized powders were characterized using scanning electron microscopy, x-ray diffraction, energy dispersive spectroscopy and charge/discharge testing. The effect of aluminium doping on the discharge capacity was studied for different aluminium concentration x= 0, 0.05, 0.1 and 0.5. The as-synthesized Al doped samples $LiAl_{0.05}Mn_{1.95}O_4$ and $LiAl_{0.1}Mn_{1.9}O_4$ exhibited higher discharge capacity for the first two cycles compared to the first cycle discharge capacity of pristine $LiMn_2O_4$. The first-principles calculations predict an increase in lattice parameter for x=0.05 and 0.1 to be responsible for the increase in first cycle discharge capacity for x=0.05 and 0.1. In addition, we have found that $LiAl_{0.5}Mn_{1.5}O_4$ sample exhibited the more stable capacity than the other samples.

Keywords: Combustion method, Al doped $LiMn_2O_4$, experimental, *ab initio* calculations, Li battery

a) Corresponding author Tel: +27 12 841 2128; Fax +27 12 841 2135.
Email: mkebede@csir.co.za

## 1. Introduction

In recent years, lithium-ion batteries have become the most promising energy sources to power the forthcoming plug-in hybrid electric vehicles or electric vehicles[1]. Lithium-ion battery (LIB) is one of the most popular types of rechargeable battery for portable electronics and power tool equipments, with the best energy densities, no memory effect, and a slow loss of charge when not in use[2-4]. $LiMn_2O_4$ spinel is a promising material for the positive (cathode) electrode in rechargeable lithium ion batteries because of its several advantages such as low cost, high abundance, low toxicity, simplicity of preparation and high safety compared with other layered oxides such as $LiCoO_2$ and $LiNiO_2$ [3,5]. However, the major problem with spinel $LiMn_2O_4$ cathode material is its rapid capacity fading upon repeated charge/discharge cycling [6,7]. Some of the causes for the capacity fade of spinel reported so far are two-phase unstable reaction [8], dissolution of spinel into the electrolyte and decomposition of the electrolyte in the 4 V region [9] and Jahn-Teller distortion[10] in the 3V region. One of strategies has been pursued to cope with this problem is substitution of small amount of trivalent Mn ions ($Mn^{3+}$) by dopant ions [6,10,11]. The dopant ions are assumed to occupy the octahedral 16d sites of Mn-ions in the spinel lattice and stabilize the spinel structure from lattice distortion [12].

Homogeneous dispersion of the $Mn^{3+}$ substituting element in crystal lattice is crucial in the synthesis of doped $LiMn_2O_4$ cathode materials. Hence, solution synthesis techniques are preferable in order to get the required homogeneously doped composition. Up to now, several solution synthesis methods have been used to synthesize $LiMn_2O_4$ spinel structured cathode material for rechargeable lithium ion batteries, such as sol-gel method [13], Pechini process [14], hydrothermal, and emulsion-drying method [15]. However, in this work we report the synthesis

of Al-doped $LiMn_2O_4$ using a solution-combustion method that allows for rapid synthesis of highly substituted oxides in a one-step process.

The conventional unit cell of cubic spinel $LiMn_2O_4$ (space group: Fd-3m #227) has 56 atoms comprised of 8 lithium (Li) atoms occupying 8a tetrahedral sites (0.125, 0.125, 0.125) and 16 manganese (Mn) atoms occupying 16d octahedral sites (0.5, 0.5, 0.5) while 32 oxygen atoms are at 32e sites (0.26, 0.26, 0.26) forming a cage as displayed in Fig.1(a). To speed up our calculations, we used the primitive cell consisting of 14 atoms, i.e. $Li_2Mn_4O_8$ shown in Fig. 1(b). Due to the dynamical Jahn-Teller distortions at $Mn^{3+}$ ions [16] which poses a challenge for the *ab initio* electronic structure calculations for mixed-valent manganese oxides, very limited first-principles investigations of $LiM_xMn_{2-x}O_4$ (M= Li, Mg, Al, Co, Ni, etc.) involving small dopant concentrations have been reported [17]. Most spin-polarized generalized gradient approximation (GGA)-based calculations, as emphasized by Mishra and Ceder [18], have been carried out only for the end compounds such as $LiMn_2O_4$ and $LiCrMnO_4$, and to certain extent $Li_xMn_2O_4$ system [19]. In transition metal substituted spinels $LiM_xMn_{2-x}O_4$ (M = transition metal), substitution is a direct replacement of the Mn atoms at their 16d positions. In the current *ab initio* calculations, we considered substitution of Mn with aluminium (M = Al) at 16d positions for x=0, 0.05, 0.1 and 0.5 compositions. The approach for the Al introduction on the Mn positions follows a solid solution mechanism described in detail elsewhere [20], based on virtual crystal approximation.

In this paper, we have synthesized $LiMn_2O_4$ and aluminium-doped spinel $LiAl_xMn_{2-x}O_4$ (for x = 0, 0.05, 0.1 and 0.5) cathode materials by solution-combustion techniques using metal nitrates and urea through exothermic and self-sustaining chemical reaction. In addition, we report the correlation between first cycle discharge capacity and lattice parameter of Al-doped spinel $LiMn_2O_4$ using experimental data analyses validated by *ab initio* calculations. The lithium

intercalation energy and electrochemical voltage of the pristine and aluminium-doped $LiMn_2O_4$ cathode materials are calculated using CASTEP total energy code [21].

## 2. Methodology

### 2.1 Experimental

$Li(NO_3)$, $Mn(NO_3)_2{\cdot}4H_2O$, $Al(NO_3)_3{\cdot}9H_2O$ and $CH_4N_2O$ with 99.9% purity were used as starting materials to synthesize $LiAl_xMn_{2-x}O_4$ cathode materials for Li ion battery. The procedure used to prepare $LiAl_xMn_{2-x}O_4$ had the following stages. The precursor metal nitrates $Li(NO_3)$, $Mn(NO_3)_2{\cdot}4H_2O$, $Al(NO_3)_3{\cdot}9H_2O$ and urea $CO(NH_2)_2$ were dissolved into deionised water and stirred at ambient temperature for about 30 min to obtain a homogeneously mixed solution. After that, the precursor solution was treated in a furnace at 500°C and black powder was obtained. To investigate the effect of Al ion on the structural and electrochemical properties of $LiMn_2O_4$ cathode materials, pristine $LiMn_2O_4$ and doped samples with Al ion concentration of 0.05, 0.1 and 0.5 were prepared under atmospheric pressure and then annealed at 700°C in air for 10 h. The voluminous and foamy combustion ash was milled to obtain the final $LiAl_xMn_{2-x}O_4$ cathode materials. The annealed samples were subjected to different morphological SEM, elemental EDS, structural XRD, and electrochemical (charge/discharge cycling) characterization.

The electrodes for electrochemical studies were prepared by making a slurry from a mixture containing active material powder, conducting black and poly(vinylidene fluoride) binder in *N*-methyl-2-pyrrolidone in the proportion 80:10:10, respectively. Coin cells of 2032 configuration were assembled using lithium metal as anode, Celgard 2400 as separator, 1M solution of $LiPF_6$ in 50:50 (v/v) mixture of ethylene carbonate (EC) and diethylene carbonate (DEC) as the electrolyte. The slurry was coated over aluminium foil and dried at 120°C for 10 h. 18 mm diameter slurry-coated aluminium foils electrodes were punched out and used as cathode.

Coin cells were assembled in an argon filled glove box (MBraun, Germany) with moisture and oxygen levels maintained at less than 1 ppm. The cells were cycled at 0.1C rate with respect to corresponding theoretical capacities of $LiAl_xMn_{2-x}O_4$ spinel and at 30°C between 2.4 and 4.8 V in an MTI a multi-channel battery tester

### 2.2 *Ab initio* calculations

First-principles calculations were carried out using CASTEP module within the Materials Studio 5.0 software package [21], which employs the plane-wave basis set to treat valence electrons and pseudo-potentials to approximate the potential field of ion cores (including nuclei and tightly bond core electrons). The CASTEP module is a first principles quantum mechanical programme based on the density functional theory formalism [22]. Spin-polarized PW91 functional of GGA [23] was employed to describe the electronic exchange-correlation interactions. Maximum plane wave cut-off energy of 500eV using Vanderbilt-type ultrasoft pseudopotentials (US) [24] and 6x6x6 Monkhorst-Pack [25] *k*-point mesh were used. Since it is now possible to use a quantum-mechanical electronic structure calculations to derive, completely from "first-principles", the voltage of a battery based on intercalation reaction energetic[26], a large amount of quantitative computational work on lithium manganese oxides (primarily $LiMn_2O_4$) have been carried out by various groups, seeking to identify suitable cathode materials for lithium batteries with guidance from first-principles calculations [27]. For cubic spinel $LiMn_2O_4$, the reaction energy of Li intercalation between two Li compositions $x_1$ and $x_2$, is given by:

$$\Delta E(x_1,x_2) = E_{tot}(Li_{x2}Mn_2O_4) - E_{tot}(Li_{x1}Mn_2O_4) - (x_2 - x_1)E_{tot}(Li, BCC) \qquad (1)$$

where $E_{tot}$ is the total energy of a system of electrons in the Coulomb potential due to the nuclei. $\Delta E$ is the energy gained upon deintercalation of Li from $LiMn_2O_4$, relative to metallic BCC Li metal. This intercalation reaction energy is simply related to the (zero temperature and pressure) open-circuit average battery voltage of a $LiMn_2O_4$/Li cell between the intercalation compositions $x_1$ and $x_2$ as shown in Eq. 2. The average open-circuit battery voltage:

$$V = -\Delta G/\Delta x F \quad (2)$$

where $\Delta x$ refers to the number of Li transferred (charge transported) and $F$ is the Faraday constant ($9.6487 \times 10^4$ C/mol). We can make a further approximation given that

$$\Delta G = \Delta E + P\Delta V - T\Delta S \quad (3)$$

where $\Delta E$, the change in internal energy, will be of the order of 0.1 – 4.0 (eV/Li atom), $P\Delta V$ is of the order of $10^{-5}$ (eV/Li atom), and $T\Delta S$ is of the order of the thermal energy ($k_BT$) which is also much smaller than ΔE at ambient temperature. Therefore the average battery voltage can be predicted by the expression

$$V = -\Delta E/\Delta x F \quad (4)$$

**3. Results and discussion**

Fig. 2(a)-(d) shows SEM images of the as-synthesized samples $LiAl_xMn_{2-x}O_4$ for x = 0, 05, 0.1 and 0.5, respectively. The particles look highly crystalline and their morphology changes with doping Al content.

Energy dispersive X-Ray Spectroscopy (EDS) elemental analysis was carried out to have an understanding of the successful aluminium doping. Though EDS cannot identify Li ions

because of its small atomic size, it helped to see the Al content in the doped samples. Fig.3 displays the EDS elemental spectra of selected samples.

A typical X-ray diffraction pattern of each sample as a function of aluminium concentration is indicated in Fig. 4. The examination of the diffraction patterns confirm that all recognizable reflection peaks including (111), (311), (222), (400), (331), (511) and (440) can be clearly indexed to the single phase of the spinel cubic structure of $LiMn_2O_4$ (JCPDS File No. 88-1749) with space group Fd-3m, without any impurity peaks. The doped $Al^{3+}$ mostly occupies octahedral Mn site (16d) [19] and enhances the cycleability by stabilizing the spinel structure. However there is an optimal amount of Al-ion doping that should maximize the structural stability of LiMn2O4.

The calculated theoretical capacity of $LiAl_xMn_{2-x}O_4$ is found to be 296 mAh/g, 284 mAh/g, 271 mAh/g, and 161 mAh/g ( assuming 1 C = 296 mA $g^{-1}$, in the voltage range of 2.4 to 4.8 V vs. Li) for x=0, x=0.05, 0.1 and x=0.5, respectively. To evaluate the electrochemical performance of the materials the charge/discharge capacity testing of the as-synthesized cathode materials was carried out at 0.1C rates with respect to their corresponding theoretical capacities.

The representative first cycle discharge capacities of $LiAl_xMn_{2-x}O_4$ (for x = 0, 0.05, 0.1 and 0.5) are presented in Fig. 5 by the curves **A**, **B, C** and **D**, respectively. During the first cycle pristine $LiMn_2O_4$ delivers discharge capacity of 136 mAh/g, $LiAl_{0.05}Mn_{1.95}O_4$ provides 159 mAh/g, $LiAl_{0.1}Mn_{1.9}O_4$ about 146 mAh/g and $LiAl_{0.5}Mn_{1.5}O_4$ gives 95 mAh/g which are comparable to their theoretical values. All the cathode samples prepared using solution-combustion method are well performing materials and delivered good first cycle discharge capacity. It was noticed that the first cycle discharge capacity for the Al-doped samples of $LiAl_xMn_{2-x}O_4$ for x = 0.05, 0.1 exhibited higher discharge capacity for the first two cycles than

that of the first discharge capacity of pristine $LiMn_2O_4$ sample as indicated in Fig 5 and Fig 6(a). To examine the possible cause(s) for the higher first cycle discharge capacity, we carried out the *ab initio* calculations on compositions corresponding to those of the experimental samples. As shown in Fig 6(b), the calculated lattice parameters of $LiAl_{0.05}Mn_{1.95}O_4$ and $LiAl_{0.1}Mn_{1.9}O_4$ respectively are 8.29Å and 8.36Å which have greater lattice parameter compared to pristine $LiMn_2O_4$ (8.28 Å). The larger the lattice parameter, the easier the Li ions can move more freely [28,29] thereby increasing the first cycle discharge capacity. This finding indicates that the discharge capacity value is not only entirely correlated to molecular weight of ion doped $LiMn_2O_4$ but also the effect of lattice parameter has to be taken into consideration. The lattice parameter of $LiAl_{0.5}Mn_{1.5}O_4$ is 8.07 Å which is smaller than the lattice parameter of the pristine $LiMn_2O_4$. Correspondingly, its first cycle discharge capacity is smaller than the first cycle discharge capacity of pristine but the cycleability is improved significantly. Corresponding to predicted lattice parameters in Fig. 6(b), the calculated open-cell voltage and intercalation energy for Li ion into the spinel cathode matrix are presented in Fig. 7 (a) and (b), respectively. The established trends indicate that introduction of Al ions results to increase in cell voltage and the more favorable energy for intercalation. As shown in figure 7, an increase in Al-dopant corresponds to more negative intercalation energy which implies easy Li ion movement. On the other hand, this increase in Al yields higher average open-circuit voltage of up to approximately 4.8 when $x = 0.5$.

Fig. 8 shows plots of the discharge capacity versus cycle number for aluminium-doped compositions ($LiAl_xMn_{2-x}O_4$) and pristine $LiMn_2O_4$ samples for the first 50cycles. Though the first cycle discharge capacity for small Al doped compounds higher than pristine $LiMn_2O_4$, the cycleability of these samples synthesized in this route is not improved. The poor cycleability of

small Al content doped samples (x=0.05 and x=0.1) is presumably $Al^{3+}$ ions substituted $Mn^{4+}$ ions instead of $Mn^{3+}$ ions that will worsen the cycleability of spinel $LiMn_2O_4$ cathode materials. On the other hand, doping with Al content of x=0.5 significantly enhanced the cycleability about 1.5times the cycleability of the pristine $LiMn_2O_4$, obviously at this time many $Mn^{3+}$ have been replaced by $Al^{3+}$ ions. Apparently, deduced from current results, $Al^{3+}$ ions seem to replace $Mn^{4+}$ ions for small Al doping concentrations resulting to increase in $Mn^{3+}$ concentration due to compatible ionic radii size of 0.535 and 0.530 Å for $Al^{3+}$ and $Mn^{4+}$ ions, respectively, hence increased lattice parameter. However, upon introducing higher amount of Al, the expected substitution of $Mn^{3+}$ (0.645Å) ions by $Al^{3+}$ ions leading to reduced ionic size mismatch between occurs $Mn^{3+}$ and $Mn^{4+}$, hence improved cycleability as a consequence of less local stresses that Li ions have to overcome. In spite of the above mechanism, the overall lattice parameter is reduced to less than that of pristine $LiMn_2O_4$, hence the lower specific capacity.

**4. Conclusion**

We have successfully synthesized $LiAl_xMn_{2-x}O_4$ (x=0, 0.05, 0.1 and 0.5) cathode materials for Li ion battery using metal nitrates and urea as precursors by solution combustion method. The samples were characterized by SEM, EDS, XRD, and battery testing and the experimental results are supported by *ab initio* computational results. The discharge capacity for the first two cycles of $LiAl_{0.05}Mn_{1.95}O_4$ and $LiAl_{0.1}Mn_{1.9}O_4$ samples is higher than that of first discharge capacity of $LiMn_2O_4$; the *ab initio* calculation shows that the lattice parameter of these compositions is greater than the lattice parameter of pristine $LiMn_2O_4$. Therefore, the *ab initio* calculation suggests that the origin for high first discharge capacities may be attributed to an increase in lattice parameter. In addition, we have found that the sample $LiAl_{0.5}Mn_{1.5}O_4$ exhibited the more stable capacity than the other samples. Similarly, the *ab initio* calculations

show that as Al content increases towards x=0.5 in the spinel cathode $LiAl_xMn_{2-x}O_4$, the composition gets more favorable energy for Li ion intercalation and increase in cell voltage.

**Acknowledgements**

The authors would like to thank CSIR for supporting this work. MK thanks NRF for the financial support with grant number 76448.

**Figure Captions**

**Fig. 1** (a) The conventional unit cell, and (b) a primitive cell of the cubic spinel structure (space group: Fd-3m) showing the different atomic positions.

**Fig. 2.** SEM images of $LiAl_xMn_{2-x}O_4$ cathode materials for (a) x=0, (b) x=0.05, (c) x=0.1 and (d) x=0.5

**Fig. 3.** Energy dispersive spectroscopy (EDS) of $LiAl_xMn_{2-x}O_4$ cathode materials for (a) x=0, (b) x=0.05 and (c) x=0.1.

**Fig. 4.** X-ray diffraction pattern of $LiMn_2O_4$ cathode materials with Al-doping concentration of (a) x=0, (b) x=0.05 and (c) x=0.1 and (d) x=0.5.

**Fig. 5.** First cycle discharge capacity curves of $LiAl_xMn_{2-x}O_4$ cathode materials **A**, **B, C** and **D** for x=0, 0.05, 0.1 and 0.5, respectively.

**Fig. 6.** (a) First cycle discharge capacity of $LiAl_xMn_{2-x}O_4$, and (b) the predicted lattice parameter of the composition $LiAl_xMn_{2-x}O_4$ (x=0, 0.05, 0.1, 0.5).

**Fig. 7.** The calculated (a) open cell voltage and (b) intercalation energy of Li ion of the composition $LiAl_xMn_{2-x}O_4$ (x=0, 0.05, 0.1, 0.5).

**Fig. 8.** The discharge capacity cycling performance of $LiAl_xMn_{2-x}O_4$ samples for the first 50cycles.

References

[1] M.M. Thackeray, C. Wolverton, E.D. Isaacs, Electrical energy storage for transportation—approaching the limits of, and going beyond, lithium-ion batteries, Energy & Environmental Science 5 (2012) 7854-7863.

[2] M. Winter, R.J. Brodd, What are batteries, fuel cells, and supercapacitors? Chem. Rev. 104 (2004) 4245-4270.

[3] A.S. Arico, P. Bruce, B. Scrosati, J. Tarascon, W. Van Schalkwijk, Nanostructured materials for advanced energy conversion and storage devices, Nature materials 4 (2005) 366-377.

[4] C. Masquelier, L. Croguennec, Polyanionic (Phosphates, Silicates, Sulfates) Frameworks as Electrode Materials for Rechargeable Li (or Na) Batteries, Chem. Rev. (2013).

[5] H. Şahan, H. Göktepe, Ş. Patat, A. Ülgen, Improvement of the electrochemical performance of $LiMn_2O_4$ cathode active material by lithium borosilicate (LBS) surface coating for lithium-ion batteries, J. Alloys Compounds 509 (2011) 4235-4241.

[6] A. Yuan, L. Tian, W. Xu, Y. Wang, Al-doped spinel $LiAl_{0.1}Mn_{1.9}O_4$ with improved high-rate cyclability in aqueous electrolyte, J. Power Sources 195 (2010) 5032-5038.

[7] M. Prabu, M. Reddy, S. Selvasekarapandian, G. Rao, B. Chowdari, (Li, Al)-co-doped spinel, Li $(Li_{0.1}Al_{0.1}Mn_{1.8})O_4$ as high performance cathode for lithium ion batteries, Electrochim. Acta (2012).

[8] W. Zhou, S. Bao, B. He, Y. Liang, H. Li, Synthesis and electrochemical properties of $LiAl_{0.05}Mn_{1.95}O_4$ by the ultrasonic assisted rheological phase method, Electrochim. Acta 51 (2006) 4701-4708.

[9] L. Xiao, Y. Zhao, Y. Yang, Y. Cao, X. Ai, H. Yang, Enhanced electrochemical stability of Al-doped $LiMn_2O_4$ synthesized by a polymer-pyrolysis method, Electrochim. Acta 54 (2008) 545-550.

[10] T. Yi, Y. Zhu, R. Zhu, L. Zhou, P. Li, J. Shu, Physicochemical properties of $LiAl_xMn_{2-x}O_4$ and $LiAl_{0.05}Mn_{1.95}O_{4-y}F_y$ cathode material by the citric acid-assisted sol–gel method, Ionics 15 (2009) 177-182.

[11] R. Thirunakaran, A. Sivashanmugam, S. Gopukumar, R. Rajalakshmi, Cerium and zinc: Dual-doped $LiMn_2O_4$ spinels as cathode material for use in lithium rechargeable batteries, J. Power Sources 187 (2009) 565-574.

[12] B. Hwang, R. Santhanam, D. Liu, Y. Tsai, Effect of Al-substitution on the stability of $LiMn_2O_4$ spinel, synthesized by citric acid sol–gel method, J. Power Sources 102 (2001) 326-331.

[13] C.J. Curtis, J. Wang, D.L. Schulz, Preparation and Characterization of $LiMn_2O_4$ Spinel Nanoparticles as Cathode Materials in Secondary Li Batteries, J. Electrochem. Soc. 151 (2004) A590-A598.

[14] S. Wu, H. Chen, The effects of heat-treatment temperature on the retention capacities of spinels prepared by the Pechini process, J. Power Sources 119 (2003) 134-138.

[15] S. Myung, S. Komaba, N. Kumagai, Enhanced Structural Stability and Cyclability of Al-Doped $LiMn_2O_4$ Spinel Synthesized by the Emulsion Drying Method, J. Electrochem. Soc. 148 (2001) A482-A489.

[16] G. Grechnev, R. Ahuja, B. Johansson, O. Eriksson, Electronic structure and magnetic properties of lithium manganese spinels, J Magn Magn Mater 258 (2003) 287-289.

[17] H. Berg, K. Göransson, B. Noläng, J.O. Thomas, Electronic structure and stability of $Li_{1+x}Mn_{2-x}O_4$ spinels, J.Mater.Chem. 10 (2000) 1437-1441.

[18] S. Mishra, G. Ceder, Structural stability of lithium manganese oxides, Physical Review B 59 (1999) 6120.

[19] H. Berg, K. Göransson, B. Noläng, J.O. Thomas, Electronic structure and stability of the $Li_xMn_2O_4$ ($0< x< 2$) system, Journal of Materials Chemistry 9 (1999) 2813-2820.

[20] M. Phasha, P. Ngoepe, An alternative DFT-based model for calculating structural and elastic properties of random binary HCP, FCC and BCC alloys: Mg–Li system as test case, Intermetallics 21 (2012) 88-96.

[21] S.J. Clark, M.D. Segall, C.J. Pickard, P.J. Hasnip, M.I. Probert, K. Refson, et al., First principles methods using CASTEP, Zeitschrift für Kristallographie 220 (2005) 567-570.

[22] P. Hohenberg, W. Kohn, Inhomogeneous electron gas, Physical Review 136 (1964) B864.

[23] J.P. Perdew, J. Chevary, S. Vosko, K.A. Jackson, M.R. Pederson, D. Singh, et al., Atoms, molecules, solids, and surfaces: Applications of the generalized gradient approximation for exchange and correlation, Physical Review B 46 (1992) 6671.

[24] D. Vanderbilt, Soft self-consistent pseudopotentials in a generalized eigenvalue formalism, Physical Review B 41 (1990) 7892.

[25] H.J. Monkhorst, J.D. Pack, Special points for Brillouin-zone integrations, Physical Review B 13 (1976) 5188-5192.

[26] Q. Ru, W. Peng, Z. Zhang, S. Hu, Y. Li, First-principles calculations and experimental studies of Sn-Zn alloys as negative electrode materials for lithium-ion batteries, Rare Metals 30 (2011) 160-165.

[27] G. Ceder, Y. Chiang, D. Sadoway, M. Aydinol, Y. Jang, B. Huang, Identification of cathode materials for lithium batteries guided by first-principles calculations, Nature 392 (1998) 694-696.

[28] Y. Huang, R. Jiang, S. Bao, Y. Cao, D. Jia, $LiMn_2O_{4-y}Br_y$ Nanoparticles Synthesized by a Room Temperature Solid-State Coordination Method, Nanoscale research letters 4 (2009) 353-358.

[29] G. Amatucci, J. Tarascon, Optimization of Insertion Compounds Such as $LiMn_2O_4$ for Li-Ion Batteries, J. Electrochem. Soc. 149 (2002) K31-K46.

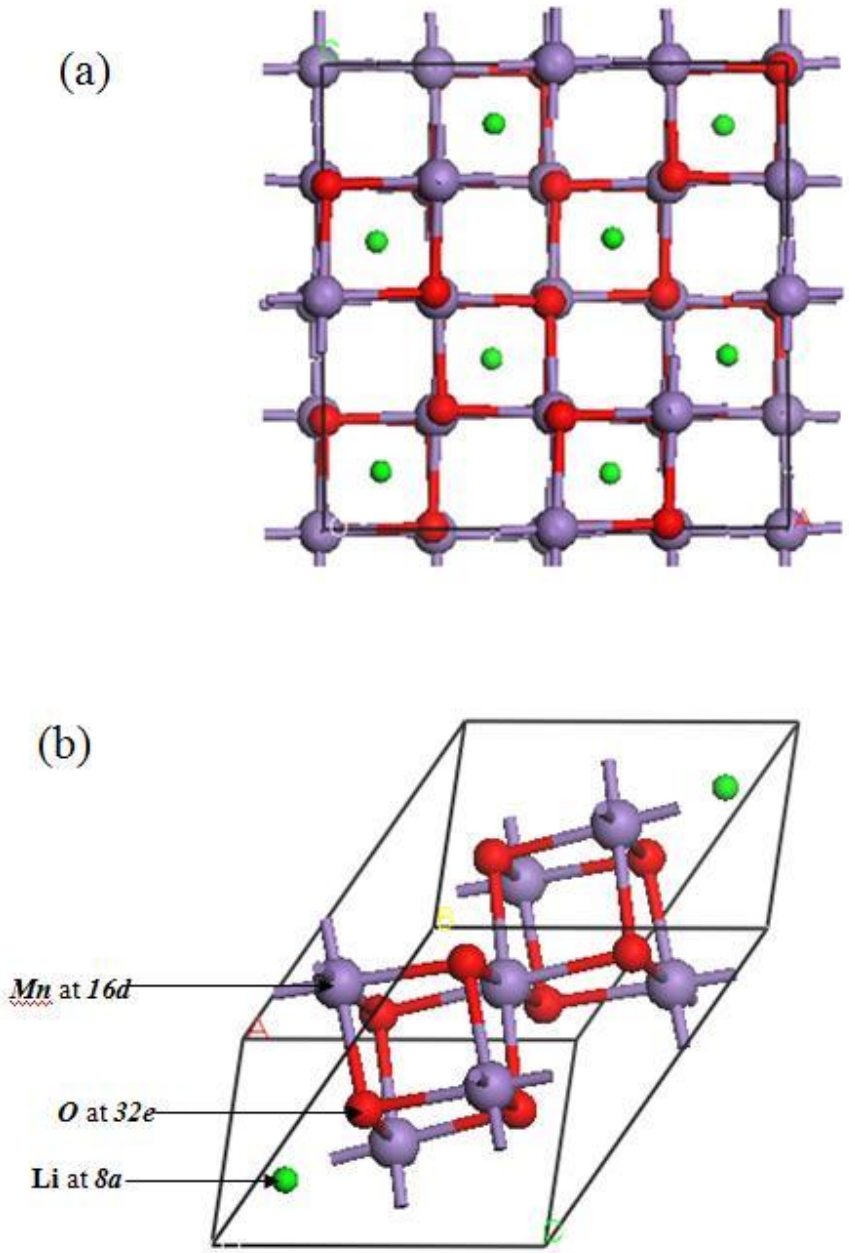


Figure 1

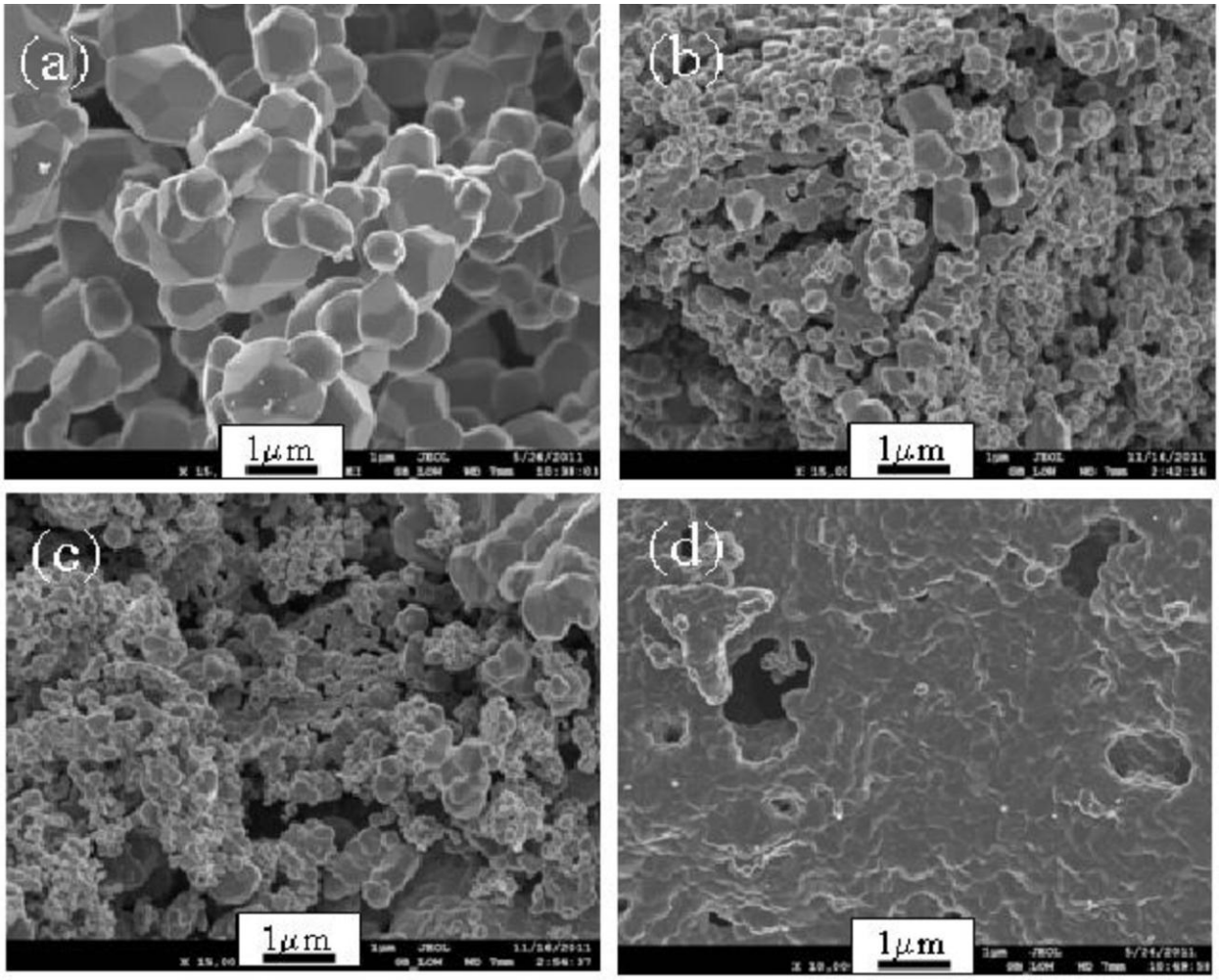


Figure 2

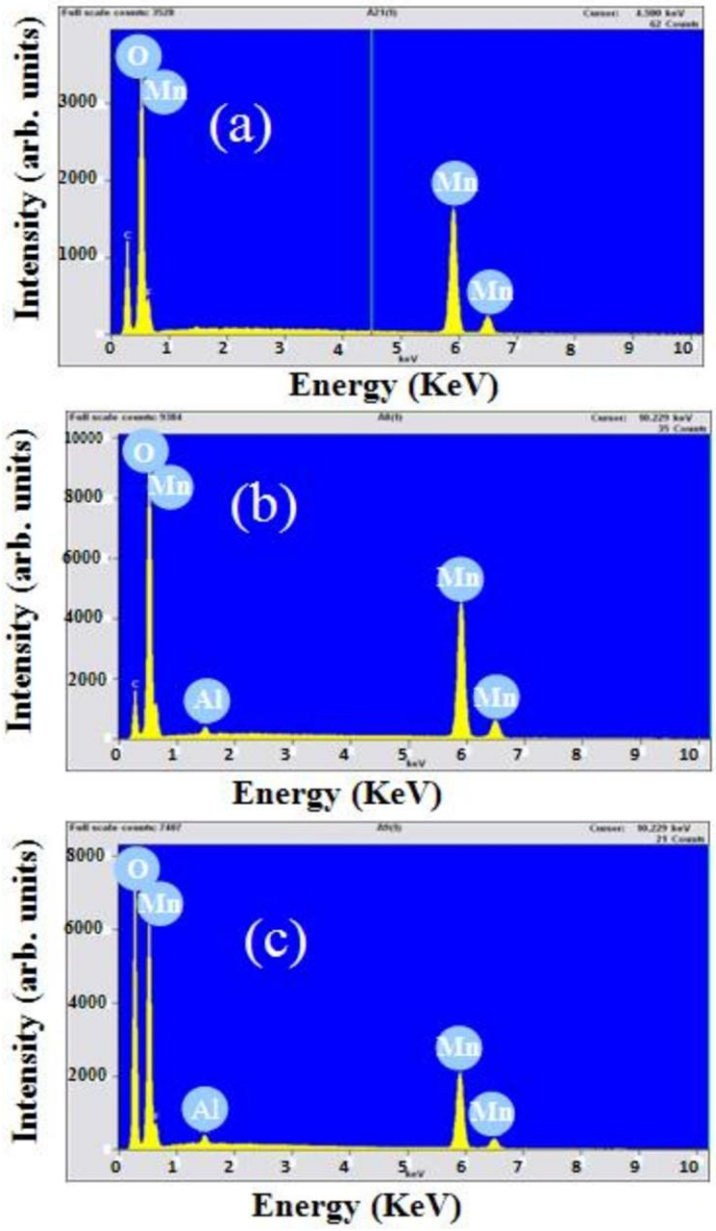
Intensity (arb. units)
(a)
O
Mn
Mn
Mn
Energy (KeV)
Intensity (arb. units)
(b)
O
Mn
Mn
Al
Mn
Energy (KeV)
Intensity (arb. units)
(c)
O
Mn
Mn
Al
Mn
Energy (KeV)

Figure 3

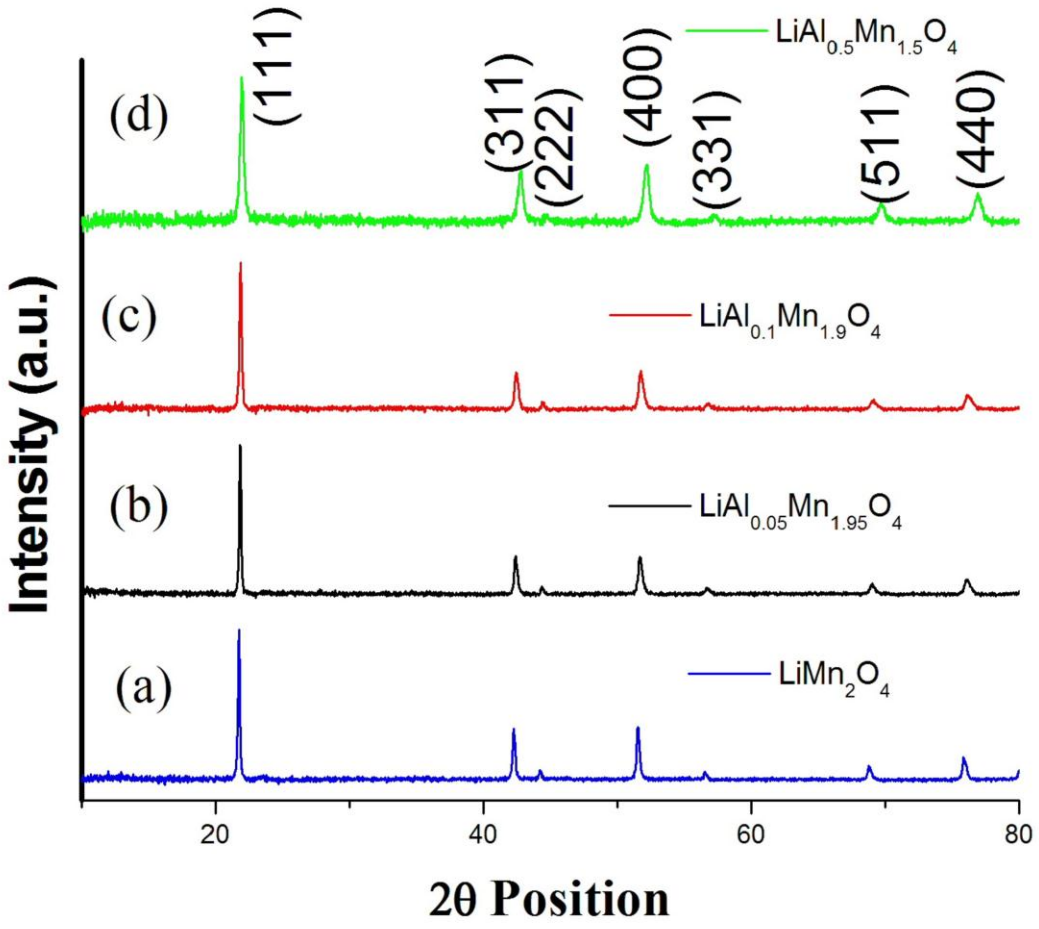
(d)
(c)
(b)
(a)
(111)
(311)
(222)
(400)
(331)
(511)
(440)
LiAl0.5Mn1.5O4
LiAl0.1Mn1.9O4
LiAl0.05Mn1.95O4
LiMn2O4
Intensity (a.u.)
20
40
60
80
2θ Position

Figure 4

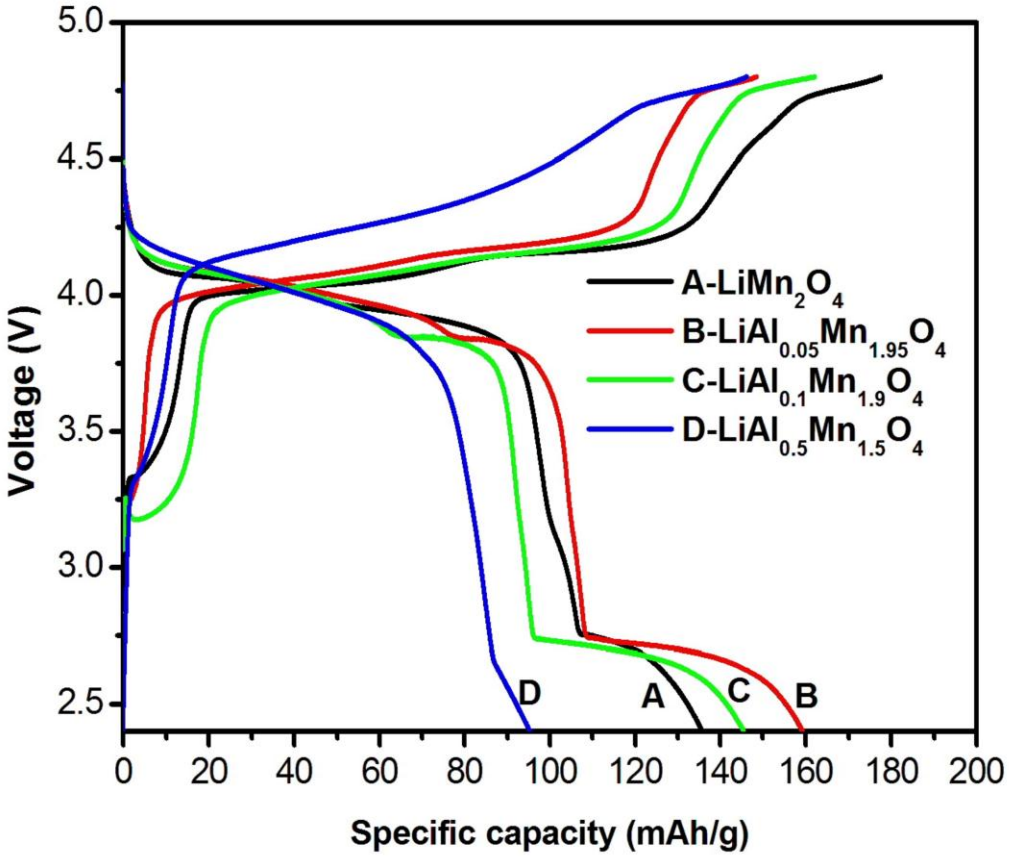
5.0
4.5
4.0
3.5
3.0
2.5
Voltage (V)
0
20
40
60
80
100
120
140
160
180
200
Specific capacity (mAh/g)
A-LiMn2O4
B-LiAl0.05Mn1.95O4
C-LiAl0.1Mn1.9O4
D-LiAl0.5Mn1.5O4
D
A
C
B

Figure 5

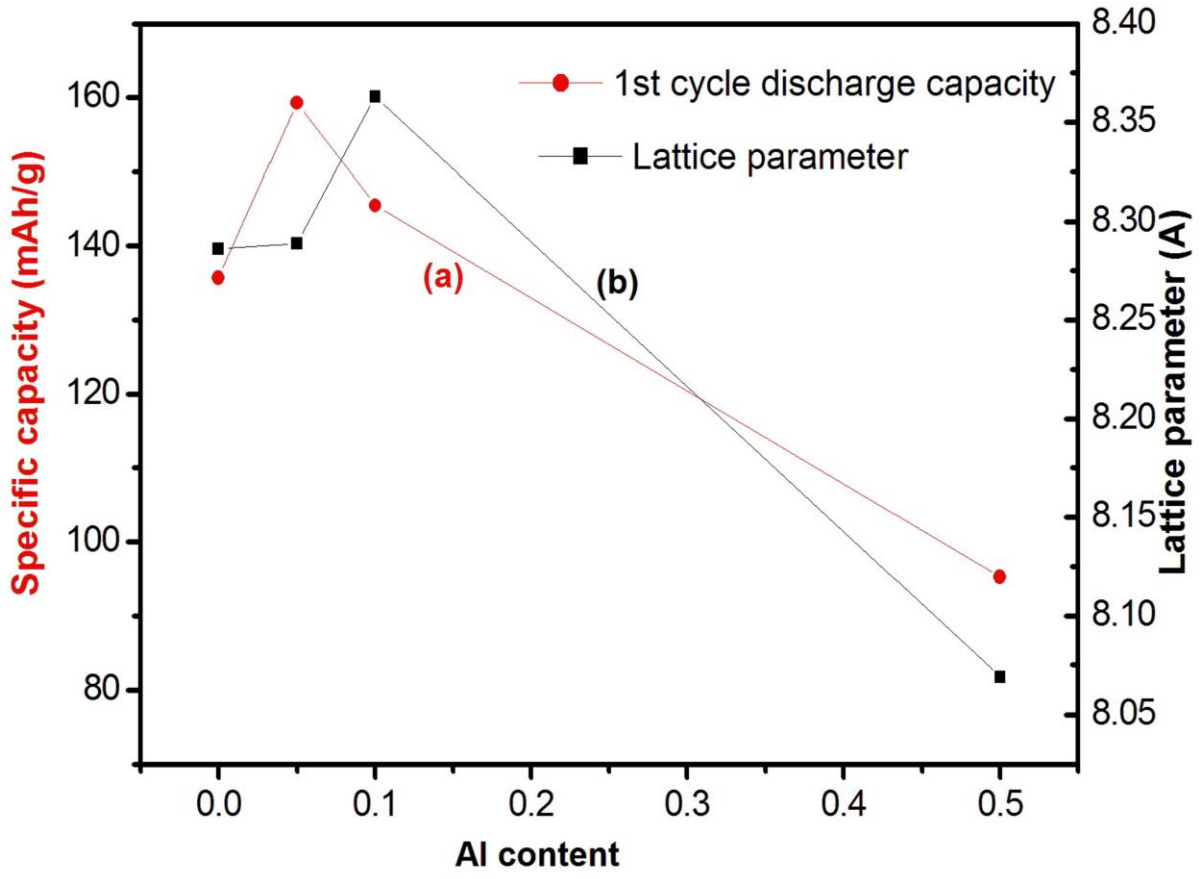
1st cycle discharge capacity
Lattice parameter
(a)
(b)
Specific capacity (mAh/g)
Lattice parameter (A)
Al content
160
140
120
100
80
8.40
8.35
8.30
8.25
8.20
8.15
8.10
8.05
0.0
0.1
0.2
0.3
0.4
0.5

Figure 6

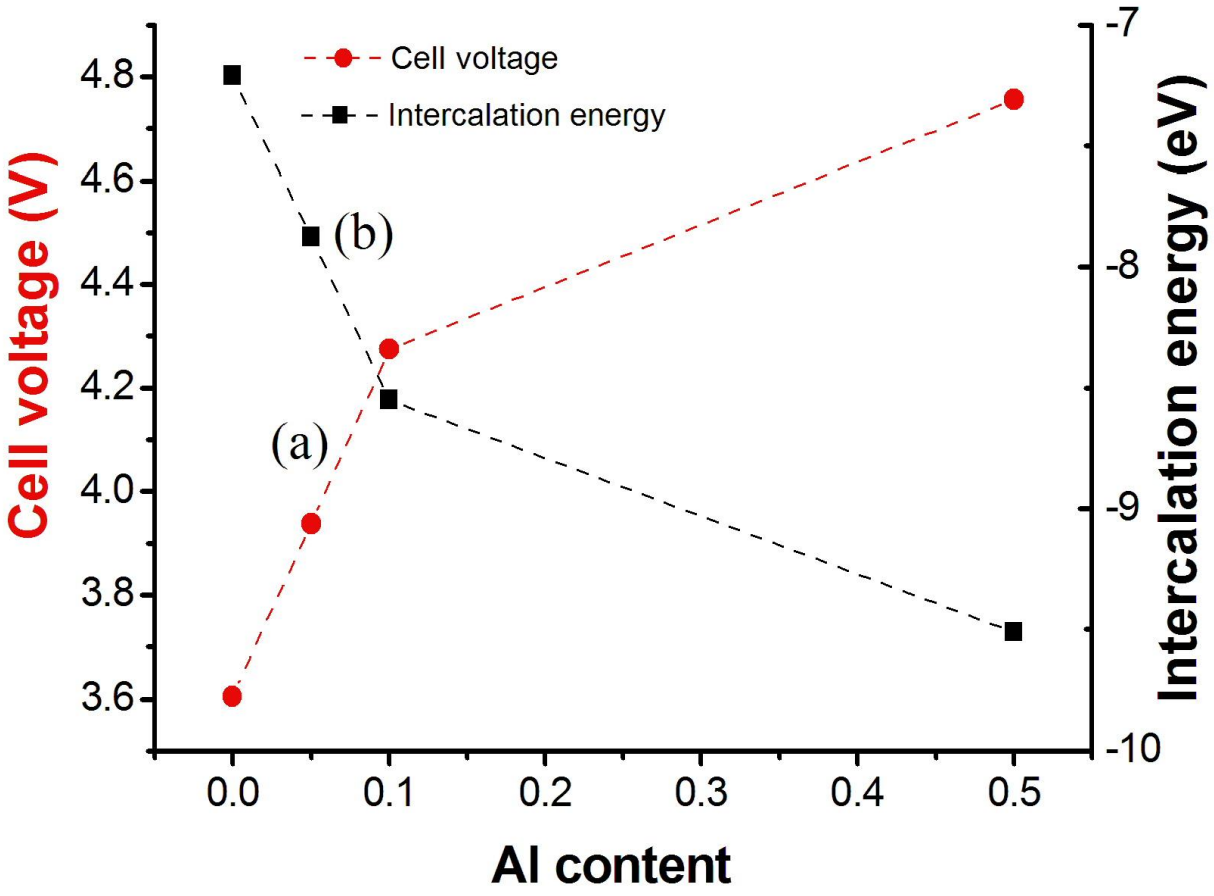
Cell voltage
Intercalation energy
(a)
(b)
Cell voltage (V)
Intercalation energy (eV)
Al content
4.8
4.6
4.4
4.2
4.0
3.8
3.6
-7
-8
-9
-10
0.0
0.1
0.2
0.3
0.4
0.5

Figure 7

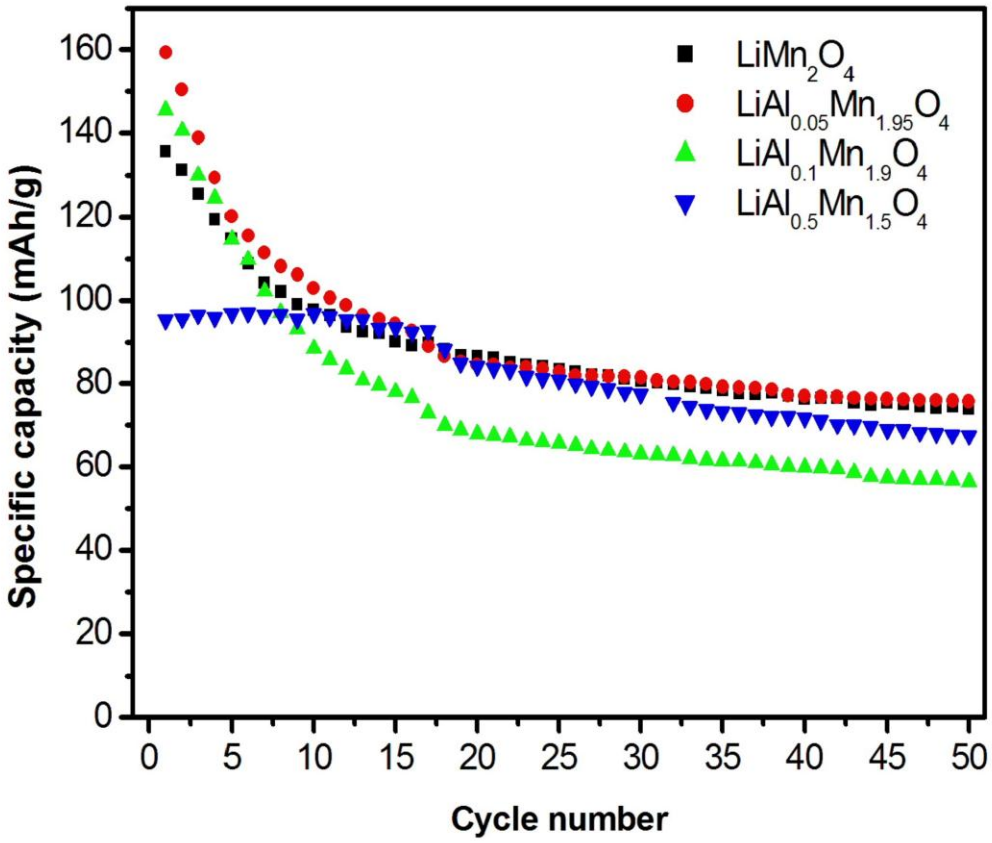
Specific capacity (mAh/g)
Cycle number
LiMn2O4
LiAl0.05Mn1.95O4
LiAl0.1Mn1.9O4
LiAl0.5Mn1.5O4
0
20
40
60
80
100
120
140
160
0
5
10
15
20
25
30
35
40
45
50

Figure 8